Interligand Electron Transfer Determines Triplet Excited State Electron Injection in RuN3−Sensitized TiO_2 Films

Gábor Benkö,[†] Jani Kallioinen,[‡] Pasi Myllyperkiö,[†,‡] Florentina Trif,[†] Jouko E. I. Korppi-Tommola,[‡] Arkady P. Yartsev,[†] and Villy Sundström[†,*]

Department of Chemical Physics, Lund University, P.O. Box 124, SE−22100, Lund, Sweden, and Department of Chemistry, University of Jyväskylä, P.O. Box 35, FIN-40014, Jyväskylä, Finland

Received: September 17, 2003; In Final Form: December 12, 2003

Electron injection from the transition metal complex $Ru(dcbpy)_2(NCS)_2$ (dcbpy = 2,2′-bipyridine-4,4′-dicarboxylate) into a titanium dioxide nanoparticle film occurs along two pathways. The dominating part of the electron injection proceeds from the initially excited singlet state of the sensitizer into the conduction band of the semiconductor on the sub-hundred-femtosecond time scale. The slower part of the injection occurs from the thermalized triplet excited state on the picosecond time scale in a nonexponential fashion, as was shown in a previous study (Benkö, G.; et al. *J. Am. Chem. Soc.* **2002**, *124*, 489). Here we show that the slower channel of injection is the result of the excited state being localized on a ligand of the sensitizer that is not attached to the semiconductor; hence, the electron cannot be injected directly from such an excited state into the semiconductor. Before being injected, it has to be transferred from the non-surface-attached ligand to the attached one. The results show that the interligand electron-transfer time is on the picosecond time scale, depends on the relative energies of the two ligands, and controls the electron injection from the excited triplet state of the sensitizer. The findings provide information relevant to the design of molecular-based assemblies and devices.

Introduction

Studying the ultrafast electron transfer (ET) from the photoexcited transition metal complex $Ru(dcbpy)_2(NCS)_2$ (RuN3; dcbpy = 2,2′-bipyridine-4,4′-dicarboxylate) to TiO_2 nanoparticles is of great significance.[1−7] The RuN3-sensitized nanocrystalline TiO_2 film (RuN3−TiO_2, Figure 1) is at the heart of the Grätzel-type dye-sensitized solar cell (DSSC), which, based on these two materials, yields an overall light-to-electricity conversion efficiency of ∼10%.[1−4]

The operation of the DSSC is directly related to the photoinduced primary processes of electron transfer at the dye-semiconductor interface. Perhaps the most essential process, the one that leads to the charge separated state, is electron injection from the photoexcited state of the dye into the conduction band of the semiconductor. Recently, our group reported that electron injection in RuN3-sensitized TiO_2 nanocrystalline films occurs on the <100 femto- and picosecond time scales.[5−7] The femtosecond part of the interfacial ET takes place from the initially excited metal-to-ligand charge transfer excited state of the RuN3, which is mainly of singlet character (called for simplicity singlet excited state, ^{1}MLCT). The picosecond part proceeds from the thermalized MLCT excited state in a nonexponential fashion.[5,6] The thermalized excited state is mainly of triplet character and is called, for simplicity, the triplet excited state (^{3}MLCT). In a similar system, RuN3-sensitized SnO_2 film (RuN3−SnO_2),[7] the pathways of electron injection are the same as in RuN3−TiO_2. The only difference between electron injection dynamics from RuN3 into TiO_2 and SnO_2 film is that the rate of singlet excited-state injection is lower for SnO_2 (1/145 fs^{-1} versus 1/55 fs^{-1}),[7]

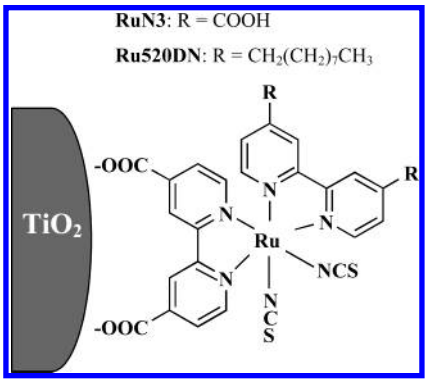

Figure 1. Molecular structures of the Ru(II)−polypyridyl complexes. The carboxylate groups ensure efficient adsorption of the dye on the TiO_2 nanoparticle surface.

which is assumed to be the result of a lower density of acceptor states in the conduction band of SnO_2.[7,8] Despite the different conduction band energetics of the semiconductors,[8] it was remarkable to see that electron injection from the RuN3 triplet state is largely independent of the two semiconductors in the presence of CH_3CN (Figure 2, data taken from ref 7). In the same study[7] we suggested that this is probably because the intramolecular processes of RuN3, such as the electron-transfer reaction between the bipyridine ligands (interligand ET: ILET),[9−11] control the triplet channel of electron injection. When the solvent environment is changed in the system, for example, placing the RuN3−TiO_2 in ethanol (RuN3−TiO_2-EtOH), a clearly slower triplet ET is noticeable (Figure 2).[12,13]

The apparent sensitivity to solvent, noticed also by other authors,[14,15] and the independence of the semiconductor of the triplet excited state electron injection naturally raise the question

* Corresponding author. E-mail: villy.sundstrom@chemphys.lu.se.
† Lund University.
‡ University of Jyväskylä.

10.1021/jp036778z CCC: $27.50
Published on Web 02/06/2004

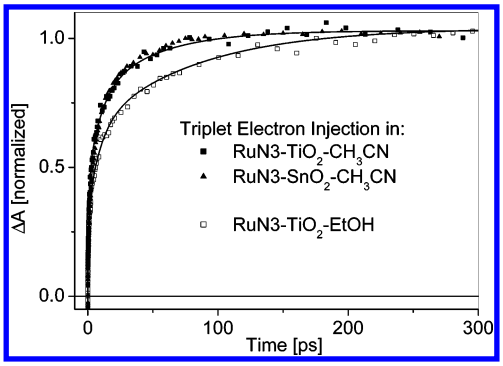

Figure 2. Kinetics of electron injection from the triplet excited state shown by the formation of the oxidized RuN3 ($RuN3^+$) at 850 nm on the picosecond time scale in RuN3-sensitized TiO_2 and SnO_2 nanocrystalline films in the presence of CH_3CN and EtOH. Note: formation of $RuN3^+$ on the <100 fs time scale is not shown in the figure. Symbols are measured data, and curves are fits to the signals with the following picosecond time constants and amplitudes: RuN3−TiO_2−CH_3CN, 1 ± 0.05 ps (38%), 10 ± 0.5 ps (35%), 50 ± 5 ps (27%); RuN3−TiO_2−EtOH, 1 ± 0.05 ps (26%), 10 ± 0.5 ps (33%), 80 ± 5 ps (41%).

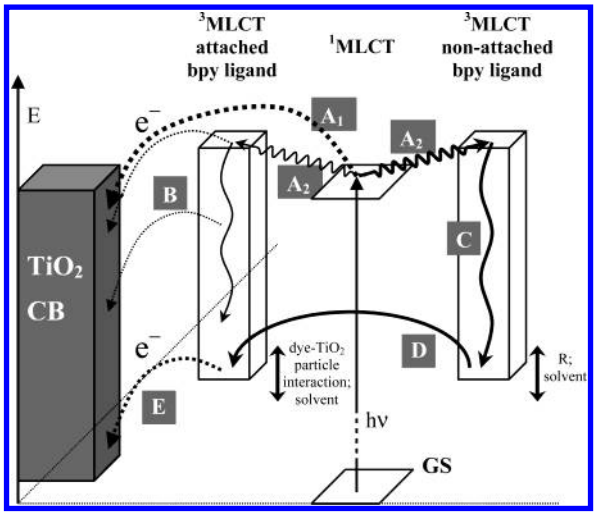

Figure 3. Schematic model for electron injection of RuN3. Following MLCT excitation of the RuN3-sensitized TiO_2 nanocrystalline film, electron injection occurs from both excited states of the dye, ^{1}MLCT and ^{3}MLCT, into the conduction band (CB) of the semiconductor. GS: ground state of RuN3. Pathway A_1: electron injection from the initially excited delocalized ^{1}MLCT excited state. Pathway A_2: ISC and localization in the ^{3}MLCT excited state. Pathway B: electron injection from the hot ^{3}MLCT excited state of the attached bipyridine ligand (not observed in the present study). Pathway C: internal vibrational relaxation in the ^{3}MLCT excited state of the nonattached bipyridine ligand. Pathways D and E: ILET between the bipyridine ligands and ensuing electron injection.

of what parameters of the system influence the electron injection. Could it be that the origin of the above-mentioned nonexponential data is in the intramolecular processes of RuN3? Or, alternatively, the binding geometry of the dye molecule on the semiconductor particle surface is a key factor. In the present work, we have performed femtosecond transient absorption polarization measurements on TiO_2 and SnO_2 films sensitized by RuN3 and Ru520DN ($RuLL'(NCS)_2$: L = 2,2′-bipyridine-4,4′-dicarboxylate, L′ = 4,4′-dinonyl-2,2′-bipyridine) to distinguish between electron injection and ILET and reveal the role of ILET in the overall electron injection dynamics of RuN3. We will use the schematic energy level diagram of Figure 3 to discuss our findings.

The key feature of our injection model is the attachment of the RuN3 molecule via two carboxylate groups of the same bipyridine ligand to the TiO_2 nanoparticles of the film. The resulting scenario is that the majority of the excited molecules inject electrons from the initially excited delocalized ^{1}MLCT state into the conduction band of the TiO_2 (pathway A_1) on the <100 fs time scale. In concert with this, the remaining population undergoes intersystem crossing (ISC), and localizes in the ^{3}MLCT state (pathway A_2). After relaxation to the bottom of the triplet state (pathway C), and interligand electron transfer (ILET, pathway D), the electrons are injected from the ^{3}MLCT state of the attached ligand (pathway E). This pathway of electron injection is controlled by ILET, which proceeds with different picosecond time constants depending on the dye molecule−TiO_2 particle interaction and solvent environment. We see no experimental evidence for electron injection from the hot ^{3}MLCT state of the attached ligand (pathway B), but on the basis of our data we cannot exclude that some injection occurs along this path. Thus, if there is any, it occurs on a time scale similar to ^{1}MLCT injection. In total, up to 70% of the ET takes place on the femtosecond time scale. The presentation and discussion of the results will be conducted below in the following order: first, the attachment of the RuN3 dye to the nanocrystalline TiO_2 film will be discussed; second, ILET in dye in solution will be characterized; and finally, we will show how ILET in the dye-sensitized films controls the electron injection from the triplet excited state of the dye localized on the non-surface-attached bipyridine ligand.

Results and Discussion

Attachment of the RuN3 Dye to the Nanocrystalline TiO_2 Film. The binding geometry of the RuN3 dye has been the subject of intense research, and several studies were reported.[16−22] Most authors seem to agree that the RuN3 dye binds to the anatase TiO_2 nanoparticle via two of its four carboxylate functional groups (Figure 1). Some authors,[19,20] employing crystallographic data, morphological examination of the TiO_2, and molecular modeling, concluded that the surface attachment of the dye occurs via two carboxylate groups that are located on different bipyridine ligands. According to these studies, the attachment of two carboxylate groups located on the same bipyridine ligand is of small probability, because of steric reasons. Contrary to this, other works[17,21,22] based on electron spectroscopy and calculations suggested that binding of the RuN3 on TiO_2 nanoparticles via two carboxylate groups of the same bipyridine ligand (as shown in Figure 1) is possible if the ligand is moderately flexible. The quantum chemical calculations showed that the modest twist of the two pyridine rings, necessary for the two carboxylate groups on the same ligand to attach, is achievable without affecting the structure of the molecule.[21]

To differentiate between the two modes of RuN3 adsorption to TiO_2 surface that were previously reported, we investigate the Ru520DN-sensitized ($RuLL'(NCS)_2$: L = 2,2′-bipyridine-4,4′-dicarboxylate, L′ = 4,4′-dinonyl-2,2′-bipyridine) TiO_2 film (Ru520DN−TiO_2). The Ru520DN dye is a modification of RuN3.[23−25] This amphiphilic sensitizer was recently synthesized[23−25] and shows similar performance[26] to RuN3 in DSSCs but with better thermal stability.[24] Compared to RuN3, the replacement of two carboxylate groups by hydrocarbon chains limits the adsorption of Ru520DN to TiO_2 film to the case when up to two carboxylates located on the same bipyridine ligand can be attached (Figure 1).[3,23−25,27] For this reason, the Ru520DN−TiO_2 couple serves as a good model system for RuN3−TiO_2. The steady-state absorption spectra of the two dyes attached to TiO_2 nanocrystalline films, prepared according to the same procedure, are shown in Figure 4. The two spectra

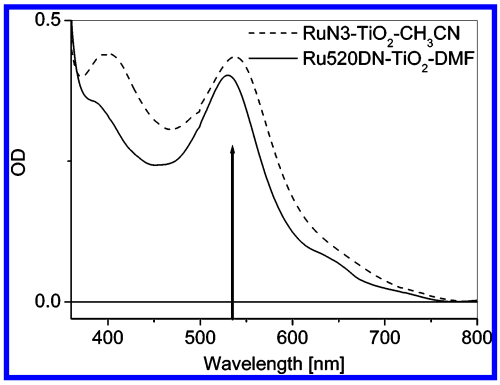

Figure 4. Steady-state absorption spectra of nanocrystalline TiO_2 films sensitized by RuN3 (dashed line) and Ru520DN (solid line), covered with CH_3CN and DMF, respectively. The arrow indicates the wavelength of laser excitation at 530 nm in the time-resolved experiments.

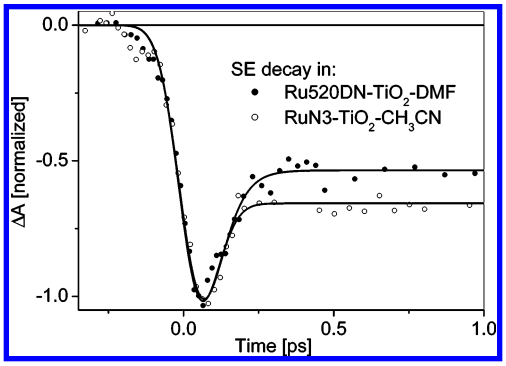

Figure 5. Kinetics of electron injection from the ^{1}MLCT excited state (decay of SE) in RuN3−TiO_2−CH_3CN at 600 nm and in Ru520DN−TiO_2−DMF at 570 nm. Symbols are measured data, and curves are fits to the signals. See text for details.

are very similar but slightly shifted. This results in a somewhat different transient absorption spectrum for Ru520DN−TiO_2 when compared to RuN3−TiO_2. In this paper, only a limited number of kinetics monitoring the interfacial electron injection in the Ru520DN-sensitized TiO_2 film are presented. The detailed femtosecond transient absorption study will be published elsewhere.[28]

The electron injection from the initially prepared ^{1}MLCT excited state of the dyes into TiO_2 can be easily followed by recording the dynamics of the stimulated emission (SE) signals.[5,6] The kinetics (Figure 5) were measured with ∼100 fs laser pulses and show instantaneous formation of the negative signal followed by a fast recovery within the laser pulse to a constant level.

The signals do not return to zero on the picosecond time scale because of the residual ground-state bleach that is present at these time delays in this spectral region. Our previous measurements with higher temporal resolution showed that SE in RuN3−TiO_2 decays with a time constant of ∼30 fs.[5,6] Hence, the data in Figure 5 show that for both dyes the electron injection from the ^{1}MLCT state occurs on the <100 fs time scale. The electron injection from the ^{3}MLCT state of Ru520DN can be monitored by the formation of the oxidized Ru520DN dye (Figure 6).[24,28] Similarly to the formation of $RuN3^+$ (Figure 2), the kinetics of $Ru520DN^+$ is also nonexponential. A fit with time constants similar to those used in Figure 2, yields a higher amplitude for the slower picosecond time constants, implying that the overall rate of triplet electron injection is slower in Ru520DN−TiO_2 than in RuN3−TiO_2. According to previous studies,[8,15] this is indeed expected. The Ru520DN dye should have a less negative excited-state redox potential than RuN3,[24,25]

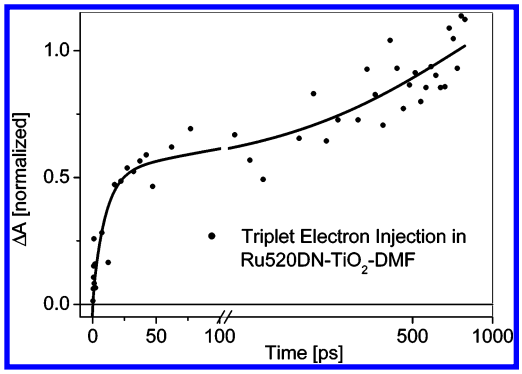

Figure 6. Kinetics of electron injection from the ^{3}MLCT excited state (formation of $Ru520DN^+$ on the picosecond time scale) in Ru520DN−TiO_2−DMF at 740 nm. Note: formation of $Ru520DN^+$ on the <100 fs time scale is not shown in the figure. Symbols are measured data, and curves are fits to the signals with the following picosecond time constants and amplitudes: 1 ps (<10%), 10 ps (∼35%), >500 ps (>55%).

which corresponds to fewer electron accepting levels to be available in the TiO_2, and may lead to slower electron injection.[8,15]

As presented above, several characteristics of the RuN3− and Ru520DN−TiO_2 systems that are expected to differ with the adsorption of the dyes to the TiO_2 surface show great similarities. The similar molecular structures of RuN3 and Ru520DN (Figure 1), the comparable adsorbed amount of dye to the same TiO_2 film (Figure 4), the identical performance in DSSCs,[23−26] the existence of two pathways for electron injection with dynamics well separated in time, the similar rates of singlet electron injection (shown above), and the similar rate for charge recombination[24] all suggest that both dyes are adsorbed most likely in the same way to the TiO_2 film, i.e., via only one bipyridine ligand, as suggested by some of the previous studies.[17,21,22]

ILET in RuN3 in Solution. When the RuN3 molecule is in solution, both of its bipyridine ligands are in contact with solvent and have similar energies. Following MLCT excitation and intramolecular energy relaxation processes in the molecule, the charge in the thermalized ^{3}MLCT excited state is localized on one of the ligands on the subpicosecond time scale, similarly to what was observed for a similar Ru-complex.[29] After localization takes place, equilibration of population between the two bipyridine ligands of the molecule, i.e., ILET, may occur.[9−11] Because ILET only induces solvent reorganization of the structurally equivalent ligands, it results in no change in transient absorption signal. Its dynamics can be revealed using time-resolved absorption polarization spectroscopy.[9,11] The ILET dynamics of RuN3 in acetonitrile solution was shown to occur on the <100 ps time scale.[10] For a similar transition metal complex $[Os(bpy)_3]^{2+}$ in solution, ILET has been demonstrated to occur with a time constant of ∼8 ps.[11] In the case of $[Os(bpy)_3]^{2+}$ with asymmetric ligands, i.e., the different ligands were differently substituted and had different energies and consequently different affinities for the electron, ILET was faster by a factor of ∼5.[11]

The time dependence of the transient absorption anisotropy of RuN3 in ethanol solution (RuN3−EtOH) is shown in Figure 7. For this system no ET product is formed; hence the only channel of deactivation of the photoexcited ^{1}MLCT state is ISC. This process, studied earlier by our group, occurs with a time constant of ∼65 fs and is reflected by the initial change in the anisotropy.[7] The faster deactivation of the singlet excited state in RuN3−TiO_2, when compared to RuN3−EtOH (inset of

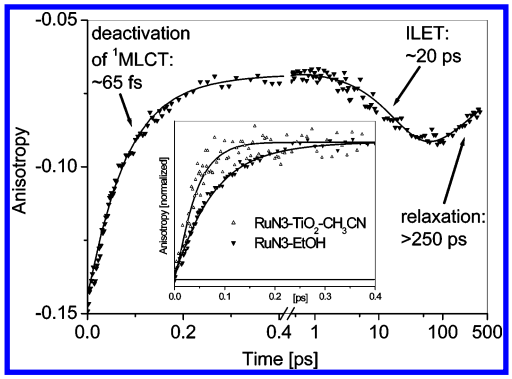

Figure 7. Time dependence of the absorption anisotropy of RuN3 in EtOH solution at 850 nm. Inset: the same data at early times together with the scaled absorption anisotropy of the RuN3-sensitized TiO_2 film. Symbols are measured data, and curves are fits to the signals with the following time constants: RuN3−EtOH, 65 ± 10 fs, 19 ± 2 ps, and >250 ps; RuN3−TiO_2−CH_3CN, 30 ± 10 fs.

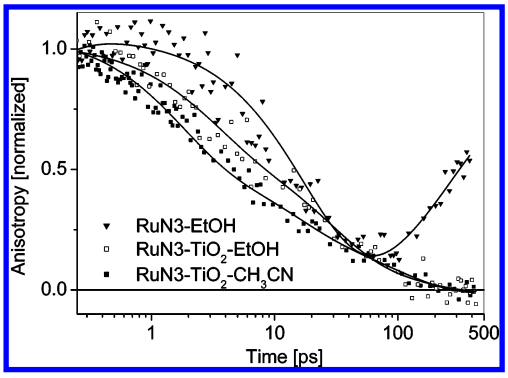

Figure 8. Time dependence of the scaled absorption anisotropy of RuN3−EtOH, RuN3−TiO_2−EtOH, and RuN3−TiO_2−CH_3CN at 850 nm, shown between 0.3 and 500 ps. Symbols are measured data. Curves, taken from Figures 2 and 7, are fits to the signals.

Figure 7), is a result of the efficient electron injection from the ^{1}MLCT state in RuN3−TiO_2. At longer delay times (>1 ps), when the molecule has already relaxed to its triplet state,[7,30] the amplitude of the anisotropy signal first increases with a time constant of ~20 ps to more negative values and later starts decaying (Figure 7). This last process is very slow compared to the previous ones, and it was measured only up to ~500 ps. Similar long time behavior was seen for the RuN3−TiO_2 samples (see below), which means that this slow (>100 ps) process is most likely not attributable to rotational diffusion of the molecule. It is probably reflecting a relaxation to lower lying excited states, similar to what has been observed for other transition metal complexes.[31]

The process occurring with the time constant of ~20 ps we attribute to ILET, because it is (1) an exponential process taking place on the <100 ps time scale, as recorded previously for RuN3[10] and for similar complexes,[11] (2) observable in time-resolved absorption anisotropy measurements, and not a spectral shift[13] or population decay (data not shown), (3) sensitive to surface attachment (see below), because the ligand symmetry of the molecule is broken (precisely what we expect from previous studies),[11] and (4) not caused by rotational reorientation of the molecule because it is not decaying to lower anisotropy values.[9,11] In conclusion of this part, the temporal evolution of the anisotropy between delay times of ~1 and ~100 ps shows the dynamics of ILET.

ILET and Electron Injection from the Triplet State in RuN3−TiO_2. We will now focus on the ILET dynamics in RuN3−TiO_2 in two solvents (CH_3CN and EtOH) and show how ILET controls the electron injection from the triplet state of RuN3 (pathways D and E in Figure 3). In RuN3−TiO_2 the two bipyridine ligands are not energetically as similar as they are for RuN3−EtOH. One of them is attached to the TiO_2 nanoparticle and its energy is influenced by the particular nanoparticle−dye molecule interaction. The other bipyridine ligand is in contact with solvent and its energy is determined by this interaction. As a result of MLCT excitation of RuN3−TiO_2 the triplet excited state will be either localized on the surface-attached ligand or on the non-surface-attached one. When the first case is realized, ILET does not influence the ET and the electrons can be injected at any moment from the excited state into the TiO_2 (pathway B in Figure 3). Because of the rapid decrease in density of conduction band states toward the bottom of the band a faster electron injection rate is expected for the ET from the surface-attached nonthermalized triplet state than for the thermalized triplet state. Therefore, this pathway of injection will have a decreasing contribution with time to the overall amplitude of ET. Because we do not observe in our experiments any electron injection from the hot triplet excited-state localized on the attached ligand (pathway B), we conclude that, if at all, it occurs on a time scale similar to singlet ET. In case the ^{3}MLCT excited state is localized on the non-surface-attached ligand after photoexcitation, the electron may undergo ILET and be injected into the semiconductor if the relative energies of the two bipyridine ligands permit (pathways D and E). In the following we will discuss this scenario.

Figure 8 shows the time dependence of the scaled absorption anisotropy of RuN3−EtOH, RuN3−TiO_2−EtOH, and RuN3−TiO_2−CH_3CN. At delay times of ~0.3 ps the dye has already relaxed to its triplet state,[5−7] and the electron injection from the singlet state and from the triplet state localized on the attached ligand are completed. The remaining excited-state population is localized in the triplet state of the nonattached ligand and undergoes ILET on the picosecond time scale, as shown by the decay of the anisotropy signal in Figure 8. Compared to ILET in RuN3−EtOH the rate of ILET in RuN3−TiO_2, regardless of solvent, is different, because the ligand symmetry of the molecule is broken by the attachment to the semiconductor. ILET is not only faster in RuN3−TiO_2 than in RuN3−EtOH but also nonexponential. Whereas ILET in solution is well fitted with a single exponential of ~20 ps, for RuN3−TiO_2 the fit requires at least three time constants ranging from ~1 to >50 ps. As ILET depends on the relative energies of the two bipyridine ligands, and because one of the ligands is in interaction with the semiconductor, the nonexponential behavior of ILET is a result of the heterogeneous interaction between RuN3 molecules and TiO_2 nanoparticles.[8,32,33] The difference in ILET in RuN3−TiO_2 in the two solvents may originate from a variety of properties of the system that cause a solvent-induced change of the energies of the ligands and therefore influence the dynamics of ILET: (1) the protonation state of the nonattached bipyridine ligand may alter its electronic environment,[34,35] (2) the energy of the attached ligand may follow the changes in the conduction band of the semiconductor that are affected by the interaction and solvent,[36−38] and (3) the ligands have different electron affinities in the two solvents.[34,35]

The fits of ILET kinetics in RuN3−TiO_2−CH_3CN and RuN3−TiO_2−EtOH in Figure 8 are essentially the same as those of the formation of $RuN3^+$ in Figure 2, implying that the kinetics of ILET and triplet electron injection are the same. The kinetics of $RuN3^+$ formation and ILET in acetonitrile and ethanol are compared in Figure 9A,B, respectively.

Also shown in Figure 9A are the ILET kinetics of RuN3−SnO_2−CH_3CN (anisotropy at 850 nm, shown up to ~30 ps)

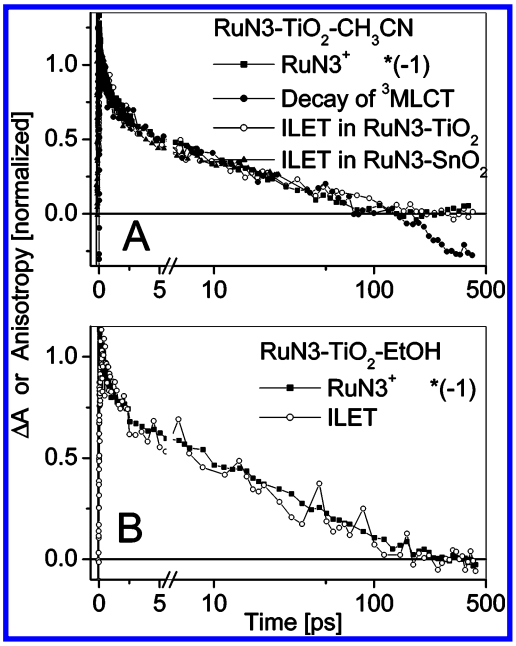

Figure 9. Comparison between the transient absorption kinetics of picosecond electron injection at 850 nm ($RuN3^+$, data from Figure 2), decay of the ^{3}MLCT state at 1050 nm, and ILET in RuN3-sensitized TiO_2 and SnO_2 films (anisotropy at 850 nm), in the presence of CH_3CN (panel A) and EtOH (panel B).

and the kinetics of RuN3−TiO_2−CH_3CN recorded at 1050 nm, the latter directly monitoring the population of the triplet state on the nonattached ligand[5,6] (the kinetics at 1050 nm in RuN3−SnO_2−CH_3CN is identical to that of RuN3−TiO_2−CH_3CN at 1050 and therefore not presented in Figure 9A). The electron injection and ILET kinetics are superimposable for both solvents and both semiconductors, showing that the population leaving the dye molecule for the semiconductor is the same as that transferred from the nonattached ligand to the attached one. *The excellent agreement between the temporal evolution of the decay of the nonattached triplet state, ILET, and picosecond electron injection from the dye molecule implies that ILET efficiently controls the triplet channel of electron injection from RuN3.*

At longer delay times at 1050 nm (>100 ps, Figure 9A), i.e., when triplet ET is completed, more long-lived dynamics of low amplitude are observed in the decay of the ^{3}MLCT state in the RuN3−TiO_2 system. The temporal characteristics of this signal are identical to the anisotropy of the dye molecules in solution at delay times >100 ps (Figure 7). Therefore, we suggest that this signal originates from a small subpopulation of noninjecting dye molecules[32,39] relaxing to lower lying excited states.[31] Because the kinetics at 850 and 1050 nm in RuN3−TiO_2 are probing different transitions in RuN3, i.e., ligand-to-metal charge-transfer transitions involving an NCS and a bipyridine ligand,[39−42] respectively, the ILET kinetics at 850 are obviously not sensitive to the noninjecting molecules.

As presented in the inset of Figure 7, the deactivation of the initially populated singlet excited state of RuN3 is considerably faster on the surface than in solution, which is a result of the efficient electron injection from the singlet excited state. Therefore, we suggest that the singlet excited state is a delocalized state, and electron injection from it occurs in concert with localization and intramolecular energy relaxation processes such as vibrational relaxation (IVR), internal conversion (IC), and ISC (pathways A_1 and A_2 in Figure 3), similarly to what has been suggested previously.[29,30] The branching ratio between the two electron injection pathways, ultrafast ET (pathways A_1 and A_2 + presumably B) and ET via the nonattached ligand (pathway E), is determined by the relative rate of electron injection from the singlet state and ISC. The scenario of population branching between the two bipyridine ligands occurring before electron injection takes place is excluded, because it would result in no difference in the rate of singlet state deactivation on the surface and in solution, contrary to the observations.

Conclusions

We have used femtosecond absorption polarization spectroscopy to investigate the interligand electron transfer (ILET) dynamics in solution and in RuN3-sensitized nanocrystalline TiO_2 films. Whereas ILET in RuN3 in solution monitors the population equilibration between the two bipyridine ligands of the dye, ILET in the dye-sensitized films shows how the electron that was promoted to the nonsurface-attached ligand is transferred to the attached one. Our measurements show that ILET occurs on the picosecond time scale, its dynamics may be altered by chemical modification of the ligands and by solvent environment and plays an important role in determining the electron injection from the triplet excited state of RuN3. On the basis of the recorded data, we propose a model that describes the electron injection in the RuN3−TiO_2 system both in time and space.

Experimental Section

1. Femtosecond Spectrometers. Time-resolved absorption measurements were conducted on the previously described 1 kHz (CLARK CPA-2001) and 5 kHz (Spectra Physics Spitfire) repetition rate amplified Ti:Sapphire laser systems.[5,6] Excitation and probe pulses both of the order of ∼25 and ∼100 fs, depending on the laser system, were generated by optical parametric amplifiers. The mutual polarization of pump and probe beams was adjusted to magic angle (54.7°) orientation. In the case of anisotropy measurements, after the beams were crossed in the sample the probe was split by a Glan polarizer to facilitate simultaneous detection of polarization components parallel and perpendicular to the pump. The accurate zero-time delay at all probe wavelengths was determined by sum-frequency cross-correlation and by the nonresonant, low-amplitude "spike-signal" in a ∼80 μm glass slide. All experiments were conducted at room temperature. Multiexponential analysis was used to quantify the recorded kinetics. Measured kinetics were analyzed with the deconvolution software Spectra Solve 2.01, LASTEK Pty. Ltd. 1997.

2. Dye-Sensitized Nanocrystalline Thin Films. RuN3 dye and TiO_2 colloidal paste (Solaronix HT) were purchased from Solaronix SA. The Ru520DN dye was a generous gift from Solaronix SA. The preparation of the SnO_2 colloidal paste is the same as that reported earlier.[7] Preparation of the dye-sensitized nanocrystalline film samples was performed according to the previously published procedure, using dye−ethanol (EtOH) solution for dye uptake.[5−7] Depending on the experiments, the samples were prepared with acetonitrile (CH_3CN), ethanol (EtOH), or dimethylformamide (DMF) immediately prior to measurements. No degradation or modification of the sample was observed in steady-state spectra recorded before and after the pump−probe measurements.

Acknowledgment. We thank Dr. Toby Meyer at Solaronix SA for the kind supply of the Ru520DN dye, Dr. Xichuan Yang and Dr. Licheng Sun at Stockholm University for characterization of the Ru520DN dye, and Dr. Wichard Beenken, Dr. Robert Smith, and Lic. Anna Szilágyi, all at Lund University, for helpful

discussions. This research was funded by grants from the Delegationen för Energiförsörjning i Sydsverige (DESS), the Swedish Research Council, the Knut and Alice Wallenberg Foundation, the Crafoord Foundation, the European Science Foundation ULTRA program, the Trygger Foundation, the Royal Physiographic Society in Lund, and the European Community under the Program "Improving Human Potential—Access to Research Infrastructures," Contract No. HPRI-CT-1999-00041.

References and Notes

(1) O'Regan, B.; Grätzel, M. *Nature* **1991**, *353*, 737−739.
(2) Nazeeruddin, M. K.; Kay, A.; Rodicio, I.; Humphry-Baker, R.; Mueller, E.; Liska, P.; Vlachopoulos, N.; Grätzel, M. *J. Am. Chem. Soc.* **1993**, *115*, 6382−6390.
(3) Kalyanasundaram, K.; Grätzel, M. *Coord. Chem. Rev.* **1998**, *77*, 347−414.
(4) Grätzel, M.; Moser, J.-E. Solar Energy Conversion. In *Electron Transfer in Chemistry*; Balzani V.; Gould, I., Eds.; Wiley-VCH: Weinheim, 2001; Vol. V, pp 589−644.
(5) Benkö, G.; Kallioinen, J.; Korppi-Tommola, J. E. I.; Yartsev, A. P.; Sundström, V. *J. Am. Chem. Soc.* **2002**, *124*, 489−493.
(6) Kallioinen, J.; Benkö, G.; Sundström, V.; Korppi-Tommola, J. E. I.; Yartsev, A. P. *J. Phys. Chem. B* **2002**, *106*, 4396−4404.
(7) Benkö, G.; Myllyperkiö, P.; Pan, J.; Yartsev, A. P.; Sundström, V. *J. Am. Chem. Soc.* **2003**, *125*, 1118−1119.
(8) Asbury, J. B.; Hao, E.; Wang, Y.; Ghosh, H. H.; Lian, T. *J. Phys. Chem. B* **2001**, *105*, 4545−4557.
(9) Waterland, M. R.; Kelley, D. F. *J. Phys. Chem. B* **2001**, *105*, 4019−4028.
(10) Olsen, C. M.; Waterland, M. R.; Kelley, D. F. *J. Phys. Chem. B* **2002**, *106*, 6211−6219.
(11) Shaw, G. B.; Brown, C. L.; Papanikolas, J. M. *J. Phys. Chem. A* **2002**, *106*, 1483−1495.
(12) Electron injection in RuN3-sensitized TiO_2 and SnO_2 films was measured in the presence of a number of different solvents. Detailed information about the solvent effects on interfacial electron injection will be presented elsewhere.[13]
(13) Myllyperkiö, P.; Benkö, G.; Kallioinen, J.; Yartsev, A. P.; Sundström, V. Manuscript in preparation.
(14) Kuciauskas, D.; Monat, J. E.; Villahermosa, R.; Gray, H. B.; Lewis, N. S.; McCusker, J. K. *J. Phys. Chem. B* **2002**, *106*, 9347−9358.
(15) Asbury, J. B.; Anderson, N. A.; Hao, E.; Ai, X.; Lian, T. *J. Phys. Chem. B* **2003**, *107*, 7376−7386.
(16) Finnie, K. S.; Bartlett, J. R.; Woolfrey, J. L. *Langmuir* **1998**, *14*, 2744−2749.
(17) Rensmo, H.; Westermark, K.; Södergren, S.; Kohle, O.; Persson, P.; Lunell, S.; Siegbahn, H. *J. Chem. Phys.* **1999**, *111*, 2744−2750.
(18) Westermark, K.; Rensmo, H.; Siegbahn, H.; Keis, K.; Hagfeldt, A.; Ojamäe, L.; Persson, P. *J. Phys. Chem. B* **2002**, *106*, 10102−10107.
(19) Shklover, V.; Ovchinnikov, Y. E.; Braginsky, L. S.; Zakeeruddin, S. M.; Grätzel, M. *Chem. Mater.* **1998**, *10*, 2533−2541.
(20) Fillinger, A.; Soltz, D.; Parkinson, B. A. *J. Electrochem. Soc.* **2002**, *149*, A1146-A1156.
(21) Persson, P.; Lunell, S. *Sol. Mater., Sol. Cells* **2000**, *63*, 139−148.
(22) Haukka, M.; Hirva, P. *Surf. Sci.* **2002**, *511*, 373−378.
(23) Wang, P.; Zakeeruddin, S. M.; Exnar, I.; Grätzel, M. *Chem. Commun.* **2002**, 2972−2973.
(24) Wang, P.; Zakeeruddin, S. M.; Moser, J. E.; Nazeeruddin, M. K.; Sekiguchi, T.; Grätzel, M. *Nature Mater.* **2003**, *2*, 402−407.
(25) Zakeeruddin, S. M.; Nazeeruddin, M. K.; Humphry-Baker, R.; Péchy, P.; Quagliotto, P.; Barolo, C.; Viscardi, G.; Grätzel, M. *Langmuir* **2002**, *18*, 952−954.
(26) Measurements performed in our laboratory showed almost identical conversion efficiencies of about 5% for the DSSCs with the dyes RuN3 and Ru520DN, employing liquid electrolyte (0.2 M LiI, 0.05 M I_2, 0.2 M 4-*tert*-butylpyridine, 0.4 M 1-hexyl-3-methylimidazolium iodide in 3-methoxypropionitrile).
(27) Lagref, J.-J.; Nazeeruddin, Md. K.; Grätzel, M. *Synth. Met.* **2003**, *138*, 333−339.
(28) Benkö, G.; Yartsev, A. P.; Sundström, V. Manuscript in preparation.
(29) Yeh, A. T.; Shank, C. V.; McCusker, J. K. *Science* **2000**, *289*, 935−938.
(30) Damrauer, N. H.; Cerullo, G.; Yeh, A.; Boussie T. R.; Shank C. V.; McCusker, J. K. *Science* **1997**, *275*, 54−57.
(31) Thompson, D. W.; Wishart, J. F.; Brunschwig, B. S.; Sutin, N. *J. Phys. Chem. A* **2001**, *105*, 8117−8122.
(32) Tachibana, Y.; Rubtsov, I. V.; Montanari, I.; Yoshihara, K.; Klug, D. R.; Durrant, J. R. *J. Photochem. Photobiol. A* **2001**, *142*, 215−220.
(33) Benkö, G.; Skårman, B.; Wallenberg, R.; Hagfeldt, A.; Sundström, V.; Yartsev, A. P. *J. Phys. Chem. B* **2003**, *107*, 1370−1375.
(34) Nazeeruddin, Md. K.; Zakeeruddin, S. M.; Humphry-Baker, R.; Jirousek. M.; Liska, P.; Vlachopoulos, N.; Shklover, V.; Fischer, C.-H.; Grätzel, M. *Inorg. Chem.* **1999**, *38*, 6298−6305.
(35) Wolfbauer, G.; Bond, A. M.; Deacon, G. B.; MacFarlane, D. R.; Spiccia, L. *J. Am. Chem. Soc.* **2000**, *122*, 130−142.
(36) Zaban, A.; Ferrere, S.; Gregg, B. A. *J. Phys. Chem. B* **1998**, *102*, 452−460.
(37) Enright, B.; Redmond, G.; Fitzmaurice, D. *J. Phys. Chem.* **1994**, *98*, 6195−6200.
(38) Lyon, L. A.; Hupp, J. T. *J. Phys. Chem. B* **1999**, *103*, 4623−4628.
(39) Tachibana, Y.; Moser, J. E.; Grätzel, M.; Klug, D. R.; Durrant, J. R. *J. Phys. Chem.* **1996**, *100*, 20056−20062.
(40) Moser, J. E.; Noukakis, D.; Bach, U.; Tachibana, Y.; Klug, D. R.; Durrant, J. R.; Humphry-Baker, R.; Grätzel, M. *J. Phys. Chem. B* **1998**, *102*, 3649−3650.
(41) Kalyanasundaram, K.; Zakeeruddin, S. M.; Nazeeruddin, M. K. *Coord. Chem. Rev.* **1994**, *132*, 259−264.
(42) Damrauer, N. H.; McCusker, J. K. *J. Phys. Chem. A* **1999**, *103*, 8440−8446.